PCCP

Accepted Manuscript

ROYAL SOCIETY OF CHEMISTRY

www.rsc.org/pccp

Cite this: DOI: 10.1039/c0xx00000x

www.rsc.org/xxxxxx

PAPER

Lasing in DNA-CTMA doped with Rhodamine 610 in butanol

T. Bazaru Rujoiu[a], A. Petris*[a] , V. I. Vlad[a], I. Rau[b], A.-M. Manea[b], F. Kajzar[b]

Received (in XXX, XXX) Xth XXXXXXXXX 20XX, Accepted Xth XXXXXXXXX 20XX
DOI: 10.1039/b000000x

The light emission properties of the complex formed by deoxyribonucleic acid (DNA) – cetyltrimethylammonium chloride (CTMA) surfactant doped with different concentrations of Rhodamine 610 (Rh610) dye and dissolved in butanol are investigated and discussed. The results are compared to those obtained when only the Rh610 is dissolved in butanol, at the same concentrations. The light emission is excited in the investigated samples by the nanosecond pulses of a frequency-doubled Nd:YAG laser, at 532 nm wavelength. We have demonstrated the lasing effect in the investigated complex and we have studied its efficiency and coherence properties. The lasing properties of the Rh610 dye are favourably influenced by the presence of the DNA-CTMA complex in the investigated compound. It leads to the increase of the lasing efficiency and of the slope efficiency. Also the temporal coherence of the emitted light is larger and the emission can be tuned to shorter wavelengths.

1. Introduction

The nowadays observed increasing application of lasers, not only in the optical signal transmission and processing, but also in medicine, industry and research demands more performant and, particularly the frequency tuned, laser sources. Some of them are dye lasers which use solutions of highly photoluminescent materials, such as e.g. rhodamines, coumarines, pyromethenes, LDS, LD, etc. (for a complete set of laser dyes see the Exciton company catalogue [1]). However these dyes degrade when subjected to high intensity pumping sources. Therefore, in practice, the lasing dye solutions are used under their continuous exchange by pumping, which requires cumbersome liquid circulation system. Also the possible dye concentrations are limited by their aggregation, leading to the photoluminescence quenching. This eventually leads to smaller lasing quantum efficiencies. Moreover, working with harmful for health and for environment solvents is not indicated. Therefore the use of solid matrices or media in which the molecules degrades slower and/or are more stable would be highly appreciated by the laser industry.

Another interesting alternative is represented by the solid dye doped lasers, in which the lasing molecules are embedded in an amorphous polymer matrix, like polymethyl methacrylate (PMMA), as it was shown a time ago [2]. Lasing materials in such lasers can be replaced easily, either for change of emission wavelength or just for replacing the degraded elements, without using solvents. Although the lack of degraded luminophore exchange, as it is the case when using solution and its circulation is a drawback for applications, some solid solutions are already in use, as exemplified by the microlasers fabricated by Teem Photonics (http://www.teemphotonics.com/). However the main problem encountered with their production and commercialization is the short lifetime of lasing media. Therefore media in which the luminophores exhibit a significantly smaller degradation time constants are highly desirable.

Recently it was shown that the deoxyribonucleic acid (DNA) - surfactant complex represents an interesting medium for photosensitive molecules, with significantly lower kinetic chemical – and photo-thermal degradation constants [3-5], as observed for synthetic polymers.

DNA biopolymer is known for its good thermal stability. This is due mainly to the base pairing between complementary strands by strong hydrogen bonds and by stacking between adjacent pairs [6]. It denatures (the process called also by melting) at ca. 90°C, passing from double into single strand helix [7] and decomposes at temperature ca. 220°C. DNA and DNA-surfactant complexes exhibit a good thermal stability and decay in the 220-230 °C temperature range [8]. The first order kinetic degradation constants k_1 for Rhodamine 590 embedded in DNA and in DNA-CTMA are of 2.78×10^{-6} min^{-1} and 1.11×10^{-6} min^{-1} at room temperature (RT) and of 6.68×10^{-6} min^{-1} and 5.0×10^{-6} min^{-1} at 85 °C, respectively, as reported by Moldoveanu et al. [3]. The decay constant k_1 increases at 85°C by a factor of ca. 2 and ca. 5 with respect to RT values. For the two studied synthetic polymers used as matrix: polycarbonate (PC) and polyethylen glycol (PEG) the corresponding values are 3.13×10^{-6} min^{-1} (PC) and 9.03×10^{-6} min^{-1} (PEG), respectively, at room temperature. These results show that Rh590 exhibits at room temperature almost the same stability in PC as in biopolymer matrices, but is less stable in PEG. At 85°C the first order kinetic degradation constants for Rh590 are four orders of magnitude larger than in biopolymers, being of 11000×10^{-6} and 8900×10^{-6} min^{-1} for PC and PEG, respectively. It shows a fast decay of luminophore in these

matrices, as compared to biopolymers.

The optical damage thresholds, which are important parameters determining the use of a given material in photonics, are higher for biopolymers. The values measured by Moldoveanu et al [4] for DNA (5.3 GW/cm^2) and DNA-CTMA (5.2 GW/cm^2) are about one order of magnitude larger than for PC (0.3GW/cm^2) and for PEG (0.78 GW/cm^2) showing that biopolymers resist better to the high energy laser pulses than the two synthetic polymers.

This better stability is probably due to the particular chemical structure of this biopolymer, which consists of a double strand helix as discovered by Watson and Crick [9, 10] in 1953. It offers a large free volume for molecules and a kind of protection for hosted photosensitive molecules. The host molecules may form an electrostatic bond with DNA, charged negatively, intercalate, fit in the major or minor groves or dope it randomly. This specific environment leads also to a higher photoluminescence quantum efficiency of embedded molecules, as compared to other matrices and reported by several research groups [11-14]. In particular an increase by a factor of 17 was observed for sulphorhodamine in DNA as compared to the PMMA matrix. The study performed by Massin et al [13] on photoluminescence of three isophorone derivatives have shown its larger quantum yield when molecules were embedded in DNA-CTMA matrix, as compared to PMMA one. Also a higher luminescence quenching concentration was observed in the biopolymer matrix. Observation of an enhancement of photoluminescence of a bio-luminophore dissolved in DNA matrix, compared to its solution was reported also by Manea et al [14].

DNA and DNA-CTMA complexes were shown already to be good matrices for lasing [15-27]. The first observation of amplified spontaneous emission (ASE), which is the laser action without cavities, and of lasing was reported by Kawabe et al [16, 22] for thin films of DNA-decyltrimethylamino (CTMA) surfactant-complex, doped with Rhodamine 590. Balan et al [20] observed ASE and lasing for the same luminophore embedded in DNA – polyvinyl alcohol (PVA) matrix. Lasing was observed for Rh590 in pure DNA matrix thin films [24]. Mitus et al [23] obtained random lasing in DNA-CTMA doped with different luminescent dyes (DCNP and Rh6G). Mysliwiec et al [21] reported ASE from thin films of merocyanine (MR) isomer of spiropyran embedded in DNA-CTMA matrix. This effect is not observed when using a synthetic polymer as matrix, such as, e.g. already mentioned PMMA. It is also absent in spiropyran (SP) form. We note here that the reversible transition from SP to MR form (and *vice versa*) is accomplished by thin film illumination by light with a corresponding wavelength to induce it. Thus a reversible memory effect can be realized with these systems, as well as, e.g. light switchable lasing systems. We note that a two photon excitation induced lasing was reported by He et al [25] for a DNA-CTMA-dye-ethanol gel. Kawabe et al [26] report also a good stability of the DMASDP bromide salt luminophore in DNA-CTMA. After two hours of lasing no remarkable damage to ASE was observed. The coherent and incoherent random lasing in polymers like DNA-CTMA and PVK doped with common laser dyes (Rh6G and DCM) was reported by Sznitko et al [27].

All these studies show that the DNA functionalized with different dyes represents a very interesting and promising material for optoelectronic and photonic applications. The specific double strand DNA helical structure, large transparency range (cutoff around 320 nm [28]), improved thermal and photothermal stability of embedded chromophores make DNA a choice material as matrix for photosensitive molecules. Chromophore molecules incorporated into the double helix grooves are efficiently prevented from aggregation, which is responsible for the intensity decrease of many optical properties. For this reason, the DNA-surfactant based host matrices seem more attractive for an extended lifetime of many devices in organic electronics and photonics, compared to classical polymer matrices such as PMMA. DNA-surfactant systems are flexible in regard to tailored properties. For example, a proper choice of the surfactant may increase or decrease optically induced birefringence [29, 30]. DNA-surfactant complexes in solid state are thermally more stable than the native DNA in solution, however less well understood processes occur during the thermal annealing [31, 32]. In fact, the complexes, like the native DNA, are compound systems that include permanently bound water [33-35]. The water cannot be removed entirely and its structural role is temperature dependent [36]. The material, if not protected, is biodegradable. This is a unique property among materials already reported to have potential applicability in the field of organic electronics and photonics, enabling straightforward recycling. The resources for obtaining DNA are renewable, as these can be the waste from the food processing industry. Thus the DNA can be cheap to obtain while contributing to the fight against pollution.

In this paper, the emission properties of DNA-CTMA complex doped with different concentrations of Rh610 (DNA-CTMA+Rh610) in butanol are investigated and compared to those of the luminophore Rh610 dissolved in butanol. The light emission in the samples is excited by pulsed frequency-doubled Nd:YAG laser. The lasing in the compound DNA-CTMA doped with Rh610 is demonstrated by the narrow spectrum and by the temporal coherence of the emitted light. The DNA-CTMA complex influences favourably the lasing properties of the Rh610 dye. The lasing efficiency and the slope efficiency are increased, the temporal coherence of the emitted light is larger and the emission wavelength can be tuned to shorter wavelengths.

2. Experimental results and discussion

2.1 Sample preparation and experimental setup

The DNA used in this study was purchased from Ogata Research Laboratory, Ltd, Chitose, Japan. It is obtained from salmon sperm. As its molecular mass is very high, it was reduced by several sonication steps. The luminophore used, Rh610, was bought at Exciton company, Dayton USA and used as supplied. The surfactant CTMA was purchased at Sigma Aldrich and also used as delivered. The chemical structures of both molecules are shown in Fig. 1.

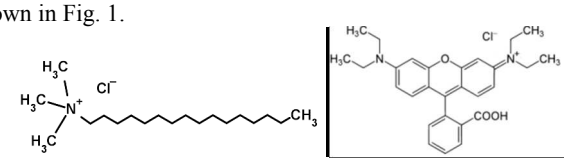

(a) (b)

Fig.1 Chemical structures of CTMA (a) and of Rhodamine 610 (b).

The DNA-CTMA complex was obtained in a similar way as described in Rau et al [37]. First a solution of DNA was prepared in 18 MΩcm deionized water after an overnight stirring at 20°C. Then the CTMA surfactant, with a slightly higher concentration was prepared in the same conditions. The solution of DNA was added drop wise to that of CTMA, also at room temperature and under stirring. The electrostatic interaction between DNA and CTMA leads to formation of a DNA-CTMA complex which precipitates in water. It was collected by filtration through a 0.4 µm nylon filter, washed with 18 MΩcm deionized water and then dried in vacuum at 35°C. The complex is soluble in water and soluble in a number of solvents, such as alcohols.

The DNA-CTMA+Rh610 complexes were prepared by solubilising dry DNA-CTMA and Rh610 at desired proportions in butanol, also under stirring at room temperature. The concentration of DNA-CTMA in butanol used was of 30 g/L and the doping concentrations of Rh610 in our samples was of 5%, 7.5%, 10%, 15% wt. The concentration represents the percentages of the dye mass with respect to the matrix dry mass. All samples have been investigated in order to observe the dependence of the emission properties on concentration. For studying the dependence of the emission properties on excitation fluence, detailed experiments have been made on samples containing Rh610 10%wt (in the middle of the Rh610 concentrations range), with and without DNA-CTMA.

The experimental setup used to study the light emission properties of the complex DNA–CTMA doped with Rh610 dye is shown schematically in Fig. 2. A frequency-doubled Nd:YAG laser (532 nm wavelength, 3 ns pulse duration, and 10 Hz repetition rate) was used as a pump laser. The pump laser beam was focused with lens L1 (f_{L1} = 150 mm) on the sample placed in its focal plane. The quartz cells containing the investigated solutions were 0.5 mm thick and their optical quality faces are plane-parallel. At this thickness the excitation beam is completely absorbed by the investigated compounds. We have measured the photoluminescence (PL) and the lasing spectra by using a spectral analyzer with fiber, Ocean Optics HR4000 CG-UV-NIR (0.5 nm resolution). In order to study the temporal coherence of the generated in the sample laser beam, it was collimated by the L2 lens and incident in a home-made Michelson interferometer. The incident beam was divided in two beams of equal intensities by the beam splitter BS. One of the mirrors (M2) can be translated along the light path in one arm of the interferometer allowing a maximum difference of 48 mm between the optical paths in the interferometer arms. The interfering beams are superimposed on the sensitive array of a laser beam analyzer connected to a computer, in order to acquire the interference patterns and to determine their visibility. The apertures A1 and A2 are introduced in the setup in order to remove the parasitic reflections. All the experiments presented in this paper were done at room temperature (~ 22°C).

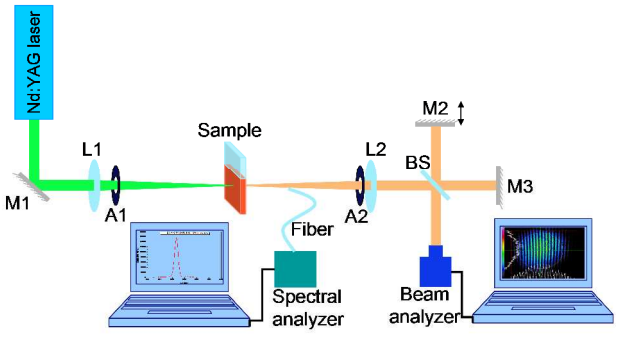

Fig. 2 The experimental setup used in light emission measurements.

2.2 The absorbance and photoluminescence properties of the samples

We have measured the absorption spectra of the samples in order to determine the proper wavelengths for the efficient excitation to get the light emission in the investigated compounds. Figure 3 shows the absorption spectra of the samples containing 10% wt Rh610, only, because the different Rh concentrations change the amplitude of the absorption spectra, but do not modify the position of the absorption peak. The absorption peak at $\lambda_{abs,\ Rh} \approx 552.5$ nm, which appears in Rh610 in butanol, is favourably shifted by several nanometers closer to the excitation wavelength of the pump laser. In the sample containing DNA-CTMA the maximum absorption wavelength is $\lambda_{abs\ DNA\text{-}Rh} \approx$ 542.6 nm. For comparison, the inset in Fig. 3 shows the absorption spectrum of DNA-CTMA in butanol. It is easy to see that, without Rh610, the DNA-CTMA in butanol compound exhibits a very low absorption at the excitation wavelength.

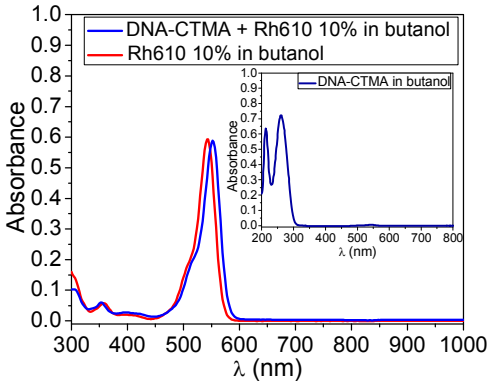

Fig. 3 Absorbtion spectra of DNA-CTMA+Rh610 10% wt in butanol and Rh610 10% wt in butanol. Inset: Absorption spectrum of DNA-CTMA in butanol.

The investigation of the emission properties of DNA-CTMA +Rh610 in butanol and Rh610 in butanol, with different concentrations of Rh610, started with the study of their photoluminescence (PL). The increase of the dye concentration leads to a red shift of PL peaks, which can be seen in the normalised PL spectra shown in Fig. 4a,b. The shift is due to the luminophore molecules aggregation and its magnitude increases with the dye concentration, as expected [38]. The effect is present in both compounds, but the difference between the wavelengths of their PL peaks decreases (Fig. 4c).

Cite this: DOI: 10.1039/c0xx00000x

www.rsc.org/xxxxxx

PAPER

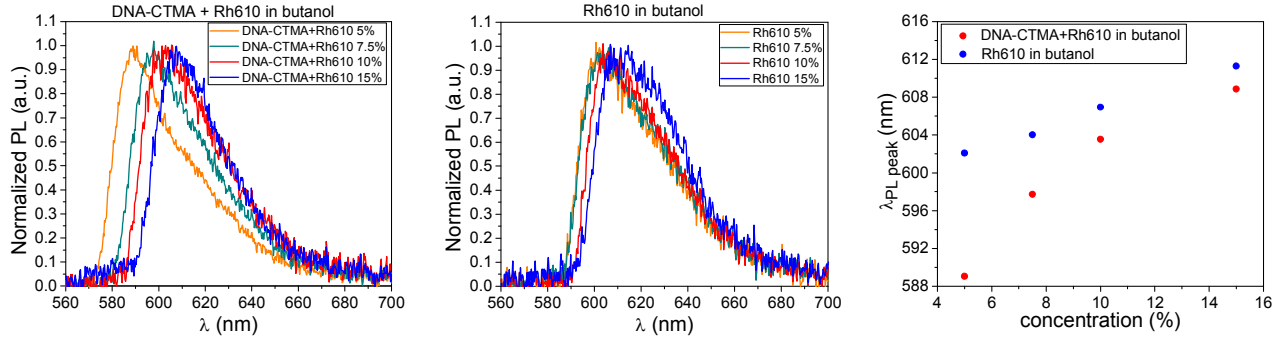

(a) (b) (c)

Fig. 4 PL spectra of DNA-CTMA+Rh610 (5%wt, 7.5%wt, 10% wt, 15%wt) in butanol (a) and Rh610 (5%wt, 7.5%wt, 10% wt, 15%wt) in butanol (b). The dependence of the PL peak wavelengths on Rh610 concentration in the samples (c)

In the range of excitation fluences used in our experiments the amplitude of PL spectra is almost proportional to the fluence of the exciting laser beam. This can be seen in Fig. 5 in which the PL spectra for the samples containing DNA-CTMA+Rh610 10% wt in butanol (Fig. 5a) and Rh610 10%wt in butanol (Fig. 5b), respectively, are shown. The amplitude dependence of PL spectra on fluence, for both compounds, is shown in Fig. 5c. In Fig. 5c one can see that the peaks of PL spectra of the sample with DNA-CTMA are less intense than those of the sample without DNA-CTMA.

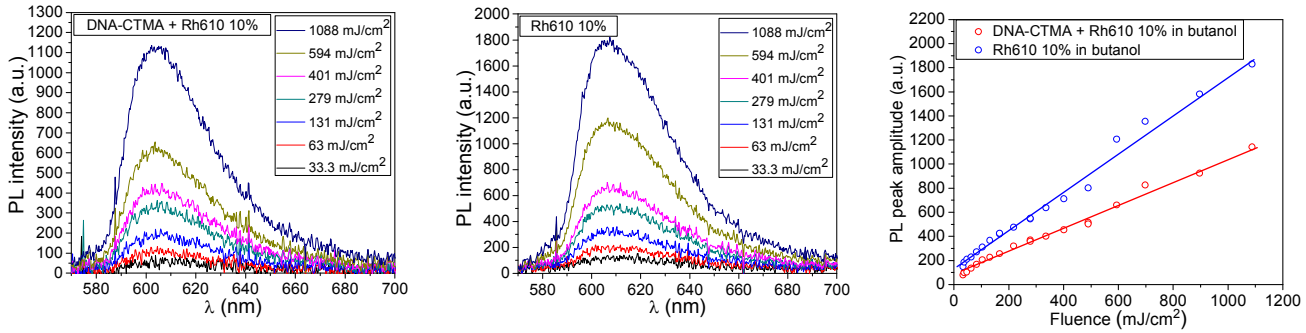

(a) (b) (c)

Fig. 5 PL spectra of DNA-CTMA+Rh610 10% wt in butanol (a) and of Rh610 10% wt in butanol (b). The dependence of the PL peak amplitude on excitation fluence for DNA-CTMA+Rh610 10%wt in butanol (red) and for Rh610 10%wt in butanol (blue), respectively (c). The continuous lines are shown for eye guiding only.

For both investigated compounds the normalization of the PL spectra reveals that their full-width at half-maximum (FWHM) is not changing when the excitation fluence is increased (Fig. 6a,b). On the other hand, the PL spectra of the samples containing DNA-CTMA are narrower than those of samples without DNA-CTMA (Fig. 6c).

Cite this: DOI: 10.1039/c0xx00000x

www.rsc.org/xxxxxx

PAPER

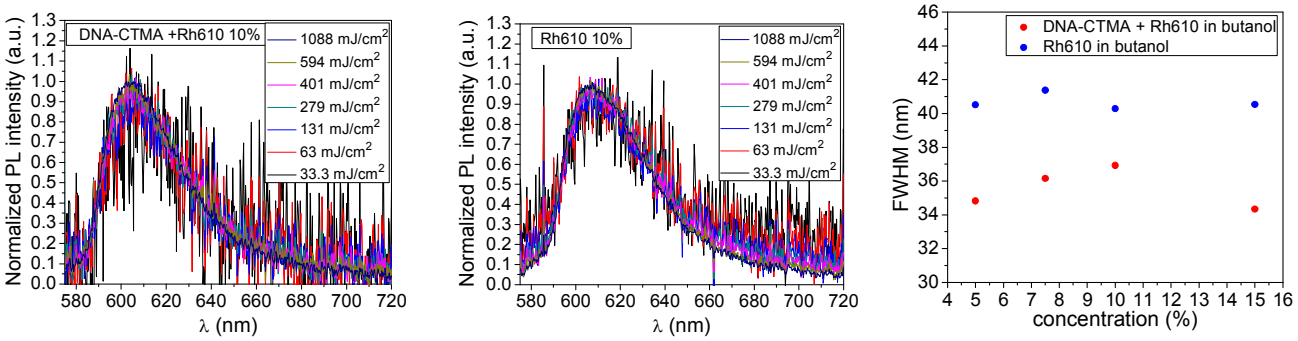

Fig. 6 Normalized PL spectra of DNA-CTMA+Rh610 10% wt in butanol (a) and of Rh610 10% wt in butanol (b). FWHM of PL spectra of DNA-CTMA+Rh610 in butanol (red) and Rh610 in butanol (blue) vs. Rh610 concentration (5%wt, 7.5%wt, 10% wt, 15%wt) (c).

2.3 The lasing effect in Rh610-doped DNA-CTMA in butanol

In this section, we present our investigations on the lasing properties of DNA-CTMA+Rh610 complex in butanol and of Rh610 alone in butanol, at the same concentrations as in the above discussed photoluminescence studies. Keeping the lateral collection of the emitted light, when the excitation fluence overcomes a certain value, a narrow peak rises from the PL spectrum, as it is shown in the Fig. 7. Due to the narrow width of the raised peaks (FWHM values range between 1.5 nm and 2.4 nm) we consider that they are associated to the laser emission in the investigated samples. For all samples these peaks occur on the left side of the PL spectra. This is different in comparison with other data reported on lasing in thin films of dye-doped DNA [17, 19, 21, 24], in which the narrow peaks appear on the right side of the PL spectra.

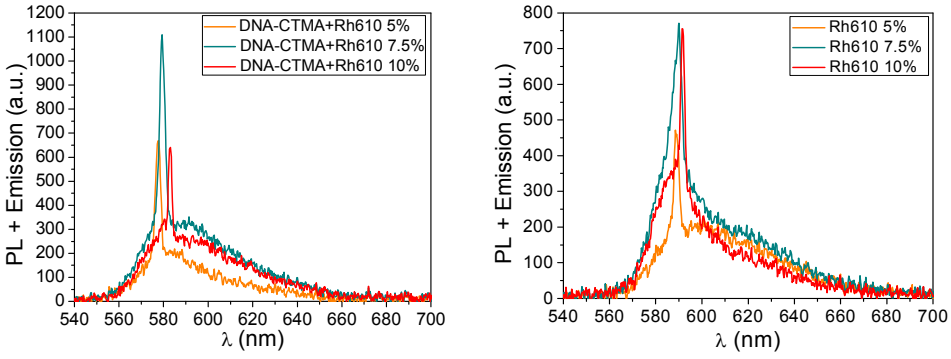

Fig.7 Lasing peaks rising from the PL spectra, for DNA-CTMA+Rh610 in butanol (a) and Rh610 in butanol (b), respectively.

In the lasing experiments the optical fiber of the spectral analyzer was placed in the back side of the cell, as shown in the Fig. 2, in order to collect the transmitted light. The lateral collection of the emitted light, used in PL measurements was chosen due to the fact that PL signal is weaker than the lasing one, making its measurement in transmission difficult, at excitation fluences higher than those for which the lasing peaks occur.

The wavelengths of the lasing peaks in the samples containing DNA-CTMA are lower compared to those in the samples containing Rh610 only (Fig. 7a,b and Fig. 8a-c). On the other hand, the wavelength of the lasing peak moves to a higher one when the Rh610 concentration is increasing. Also we notice the appearance of two lasing peaks in both samples with 15%wt of Rh610, with and without DNA-CTMA.

Cite this: DOI: 10.1039/c0xx00000x

www.rsc.org/xxxxxx

PAPER

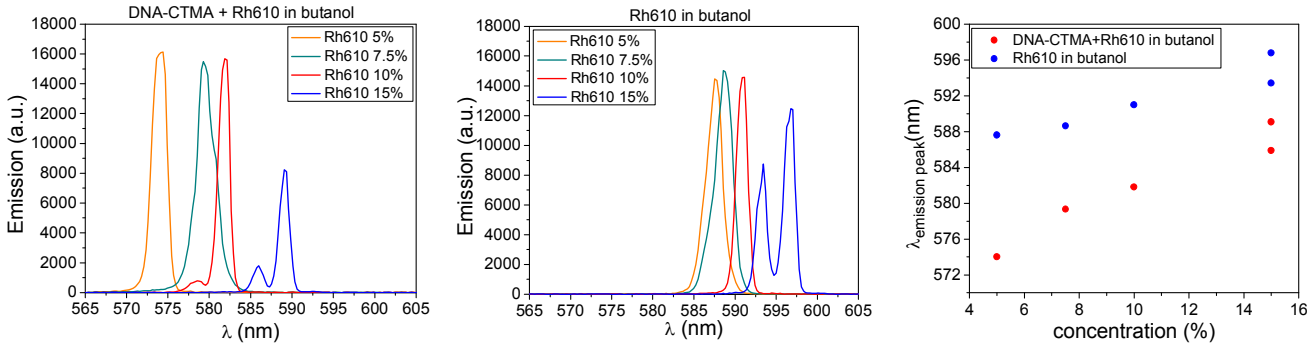

(a) (b) (c)

Fig. 8 Lasing spectra of DNA-CTMA+Rh610 (5%wt, 7.5%wt, 10% wt, 15%wt) in butanol (a) and of Rh610 (5%wt, 7.5%wt, 10% wt, 15%wt) in butanol (b); (c) Dependence of the emission peak wavelengths on the Rh610 concentration.

The lasing effect occurs at a value of the excitation fluence (threshold fluence, F_{th}) for which the stimulated emission of the photons exceeds the loss due to the scattering and absorption [21]. The threshold fluence was estimated for each sample with respect to the dye concentration (Fig. 9 (a)). In the sample DNA-CTMA+Rh610 5%wt in butanol, the lasing occurs at the threshold fluence $F_{th1} \approx 13.5$ mJ/cm^2. In the sample Rh610 5%wt in butanol, the threshold fluence is slightly higher, $F_{th2} \approx 17$ mJ/cm^2. For the other samples, with 7.5%wt, 10%wt and 15%wt dye concentration, the situation is reversed. We have obtained lasing at lower fluences in samples Rh610 (7.5%wt: 26.5 mJ/cm^2, 10%wt: 41.1 mJ/cm^2 and 15%wt: 90.1 mJ/cm^2) in comparison with the samples DNA-CTMA+Rh610 (7.5%wt: 30.7 mJ/cm^2, 10%wt: 45.8 mJ/cm^2 and 15%wt: 133.7 mJ/cm^2) (Fig. 9a). While for the samples with dye concentrations of 5%wt, 7.5% and 10%wt, containing DNA-CTMA or not, the thresholds have close values, for the samples with Rh610 15%wt the difference is higher.

The dependence of the emitted energy on excitation fluence is shown in Fig. 9 (b) for DNA-CTMA+Rh610 10%wt in butanol and for Rh610 10%wt in butanol, respectively. From this figure the optical-to-optical efficiency ($\eta = E_{emission}/E_{pump}$) and the slope efficiency of the lasing effect, defined as the slope of the linear fit of the experimental points obtained for pump fluences higher than those corresponding to the threshold, are determined. For dye-doped DNA-CTMA in butanol the efficiency increases from 0.3% to 3.4%, in the range of excitation fluences between the threshold and the maximum one used in our experiment. The corresponding slope efficiency is 4%. These values are larger than those obtained for the sample containing only Rh610 in butanol, for which the efficiency increases from 0.2% to 2.4% in the range of excitation fluences used in the experiment and the corresponding slope efficiency is 2.8%.

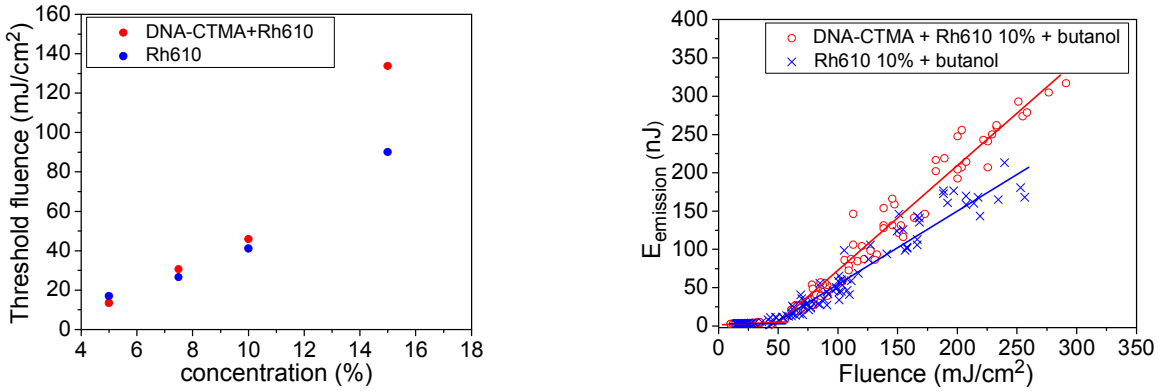

(a) (b)

Fig. 9 (a) Dependence of the threshold fluence on Rh610 concentration; (b) The lasing efficiency for DNA-CTMA+Rh610 10%wt in butanol (red) and for Rh610 10%wt in butanol (blue). The red and blue lines are the linear fit of the experimental data for dye-doped DNA-CTMA and for Rh610 10%wt, respectively.

Cite this: DOI: 10.1039/c0xx00000x

www.rsc.org/xxxxxx

PAPER

An image of the laser beam spot emitted by the Rh610-doped DNA-CTMA in butanol (yellow) and of the excitation laser beam (green), transmitted by the cell containing the investigated compound is shown in the Fig. 10. It can be seen also the PL light emitted through the lateral side of the cell (reddish). In order to take this picture, we have used a cell of 0.2 mm thickness, which allows the partial transmission of the green excitation light.

Fig. 10 Beam spots of the emitted (yellow) and excitation (green) light. It can be seen also the PL light (reddish) emitted through the lateral side of the cell containing Rh610-doped DNA-CTMA in butanol.

2.4 The coherence of the light emitted by Rh610-doped DNA-CTMA in butanol

We investigated the coherence properties of the light emitted by our samples. In these experiments we have used a Michelson interferometer (see the experimental setup, Fig. 2). The initial position of the mirror M2 is considered that for which the fringe pattern has the best visibility (equal optical paths for the light in both arms of the interferometer). Then, the optical path difference is increased by moving step by step the mirror M2 along the light propagation direction, until it is difficult to discriminate between bright and dark fringes. For each step the fringe pattern is acquired by using a laser beam analyzer connected to a computer. In each pattern we measured the maximum (I_{max}) and minimum (I_{min}) grey levels, corresponding to bright and dark fringes, respectively, and we calculated the fringe visibility: $V = (I_{max} - I_{min}) / (I_{max} + I_{min})$. When the optical path difference is equal to zero, the maximum visibility is equal to 1 for interfering beams of the same intensity and perfectly superimposed on the sensitive array of the laser beam analyzer (the interference plane). We consider the coherence length as being the optical path difference for which the fringe visibility is reduced to 1/e (= 0.37) of the maximum visibility, equal to 1 [39, 40].

In Fig. 11, we show the interference patterns at several optical path differences between the interferometer arms for the samples DNA-CTMA+Rh610 10% wt in butanol and Rh610 10% wt in butanol, respectively.

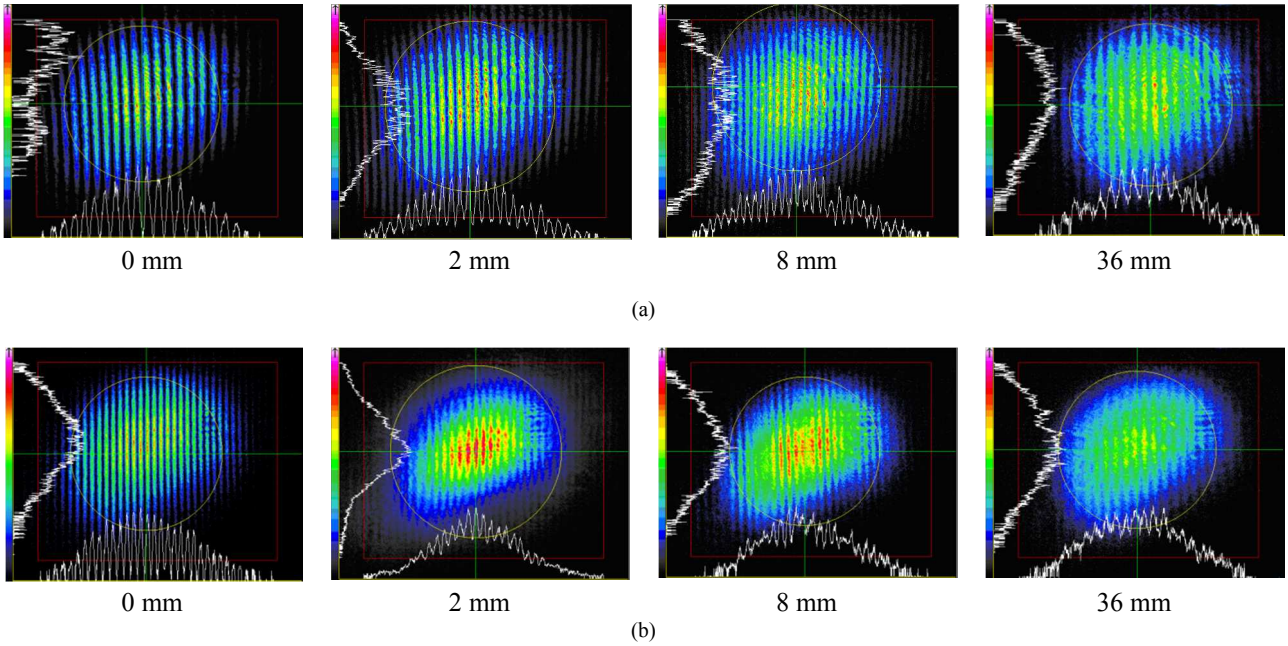

Fig. 11 The interference patterns at several optical path differences between the interferometer arms, for the samples DNA-CTMA+Rh610 10% wt in butanol (a) and Rh610 10% wt in butanol (b), respectively.

The dependence of the fringe visibility on optical path difference, for the same samples as considered in Fig. 11, is shown in Fig. 12. It can be seen that the coherence length of the laser beam emitted by the sample DNA-CTMA+Rh610 10% in

butanol is ~16 mm and is larger than that obtained for the sample Rh610 10% in butanol, where the coherence length is ~8 mm. These results reveal that adding DNA-CTMA to the solution containing Rh610 10% in butanol improves the spatial coherence of the emitted light.

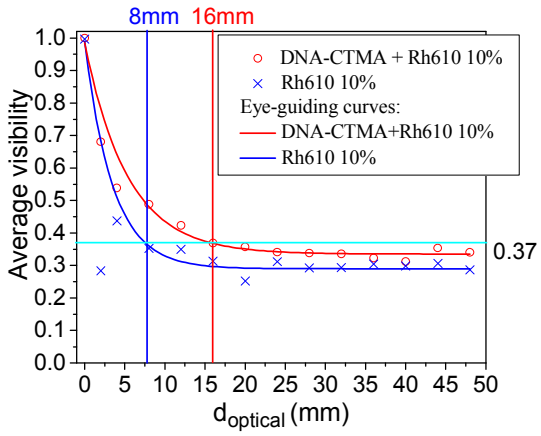

Fig. 12 The dependence of the fringe visibility on optical path difference for DNA-CTMA+Rh610 10% wt in butanol (red) and Rh610 10% wt in butanol (blue), respectively.

Conclusions

In this paper the results of our experimental comparative study on light emission (photoluminescence and lasing) in DNA-CTMA+Rh610 in butanol and Rh610 in butanol samples are presented and discussed. We demonstrated the lasing effect in the investigated compounds and we studied the influence of DNA-CTMA environment on lasing threshold, efficiency and coherence properties. In the samples with DNA-CTMA, both photoluminescence and lasing peaks occur at shorter wavelengths in comparison with the samples containing Rh610 only. The increase of the dye concentration shifts the emission peaks to longer wavelengths and leads to higher threshold fluences, in both investigated compounds. Our experiments revealed a favourable influence of DNA-CTMA on lasing emission. For DNA-CTMA samples doped with Rh610 10%, the lasing efficiency (0.3% to 3.4%, in the range of excitation fluences used in our experiment) and the slope efficiency (4%) are approximately 1.4 times higher, and the coherence length (~16 mm) is double in comparison to the samples containing the dye only.

Acknowledgements

The authors acknowledge the financial support of Romanian Ministry of National Education and Scientific Research, through the UEFISCDI, under Contract Number 3/2012, Project Code PN-II-PT-PCCA-2011-3.1-0316, “BIO-NANO-PHOTO”.

Notes and references

[a] *National Institute for Laser, Plasma and Radiation Physics, Dept. of Lasers, 409 Atomistilor Str., R-077125 Bucharest – Magurele, Romania; *Corresponding author: adrian.petris@inflpr.ro*

[b] *University POLITEHNICA of Bucharest, Faculty of Applied Chemistry and Materials Science, 1 Polizu Str., Bucharest, Romania*

1 http://www.exciton.com/laserdyeslist.html
2 O. G. Peterson and B. B. Snavery, *Appl. Phys. Lett.*, 1968, **12**, 238-240.
3 M. Moldoveanu, A. Meghea, R. Popescu, J. G. Grote, F. Kajzar and I. Rau, *Mol. Cryst. Liq. Cryst.*, 2010, **522**, 180/[480] – 190/[490].
4 M. Moldoveanu, R. Popescu, C. Pîrvu, J. G. Grote, F. Kajzar and I. Rau, *Mol. Cryst. Liq. Cryst.*, 2010, **522**, 530 – 539.
5 I. Rau, A. Tane, R. Zgarian, A. Meghea, J. G. Grote and F. Kajzar, *Mol. Cryst. Liq. Cryst.*, 2012, **554** (1), 43-55.
6 P. Yakovchuk, E. Protozanova and M. D. Frank-Kamenetskii, *Nucleic Acids Research*, 2006, **34** (2), 564–574.
7 R. D. Blake and S. G. Delcourt, *Nucleic Acids Research*, 1998, **26** (14), 3323–3332.
8 J. G. Grote, "Biopolymer materials show promise for electronics and photonics applications", *SPIE News room*, 2008, 1-5, DOI 10.1117/2.1200805.1082.
9 J. D. Watson and F. H. C. Crick, *Nature*, 1953, **171**, 737-738.
10 F. H. C. Crick and J. D. Watson, *Proc. Royal Soc. (London)*, 1954, **223**, 80-96.
11 Z. Yu, W. Li, J. A. Hagen, Y. Zhou, D. Klotzkin, J. G. Grote and A. J. Steckl, *Appl. Optics*, 2006, **46**, 1507.
12 J. A. Hagen, W. Li, A. J. Steckl and J. G. Grote, *Appl. Phys. Lett.*, 2006, **88**, 171109.
13 J. Massin, S. Parola, C. Andraud, F. Kajzar and I. Rau, *Opt. Mat.*, 2013, **35** (10), 1810-1816.
14 A.-M. Manea, I. Rau, F. Kajzar and A. Meghea, *Opt. Mat.*, 2013, **36** (1), 140-145.
15 Y. Kawabe, L. Wang, S. Horinouchi and N. Ogata, *Adv. Mater.*, 2000, **12** (17), 1281-1283.
16 Y. Kawabe, L. Wang, T. Koyama, S. Horinouchi and N. Ogata, *Proc. SPIE*, 2000, **4106**, 369 – 376.
17 J. Mysliwiec, L. Sznitko, A. Miniewicz, F. Kajzar and B. Sahraoui, *J. Phys. D: Appl. Phys.*, 2009, **42** (8), 085101.
18 M. Leonetti, R. Sapienza, M. Ibisate, C. Conti and C. Lopez, *Opt. Lett.*, 2009, **34** (24), 3764–3766.
19 L. Sznitko, J. Myśliwiec, P. Karpiński, K. Palewska, K. Parafiniuk, S. Bartkiewicz, I. Rau, F. Kajzar and A. Miniewicz, *Appl. Phys. Lett.*, 2011, **99** (3), 031107_1-3.
20 N. Balan, M. Hari and V. P. N. Nampoori, *Appl. Opt.*, 2009, **48**, 3521–3525.
21 J. Mysliwiec, L. Sznitko, S. Bartkiewicz, A. Miniewicz, Z. Essaidi, F. Kajzar and B. Sahraoui, *Appl. Phys. Lett.*, 2009, **94**, 241106_ 1-3.
22 Y. Kawabe and K.-I. Sakai, *Nonl. Opt. Quant. Opt.*, 2011, **43**, 273–282.
23 A. C. Mitus, G. Pawlik, J. Mysliwiec, L. Sznitko, K. Cyprych, A. Szukalski, F. Kajzar and I. Rau, *Proc. SPIE* , 2014, **9171**, 91710H.
24 I. Rau, A. Szukalski, L. Sznitko, A. Miniewicz, S. Bartkiewicz, F. Kajzar, B. Sahraoui and J. Mysliwiec, *Appl. Phys. Lett.* , 2012, **101**, 171113.
25 G. S. He, Q. Zheng, P. N. Prasad, J. G. Grote and F. K. Hopkins, *Opt. Lett.*, 2006, **31**, 359–361.
26 Y. Kawabe, L. Wang, T. Nakamura and N. Ogata, *Appl. Phys. Lett.*, 2002, **81** (8), 1372–1374.
27 L. Sznitko, K. Cyprych, A. Szukalski, A. Miniewicz, I. Rau, F. Kajzar and J. Mysliwiec, *Proc. SPIE* , 2013, **8901**, 89010Y.
28 I. Rau., J. G. Grote, F. Kajzar and A. Pawlicka, *Comptes Rendus Physique*, 2012, **13**, 853-864.
29 J. Mysliwiec, K. Parafiniuk, A. Miniewicz, I. Rau, F. Kajzar, J. Niziol, E. Hebda, J. Pielichowski and B. Sahraoui, *Proc. SPIE*, 2012, **8464**, 84640C-1-6.
30 L. Sznitko, K. Parafiniuk, A. Miniewicz, I. Rau, F. Kajzar, J. Niziol, E. Hebda, J. Pielichowski, B. Sahraoui and J. Mysliwiec, 2013, *Opt. Mat.*, **35** (12), 2389-2393.
31 J. Nizioł, M. Dendzik, M. Sitarz, E. Hebda, J. Pielichowski, J. Łojewska, A. Rogulska and M. Bakasse, *Opt. Mat.*, 2013a, **36** (1), 36-41.
32 J. Nizioł, *J. Appl. Phys.*, 2014, **11** (23), 234701.
33 H. Haranczyk, J. Kobierski, D. Zalitacz, P. Nowak, A. Romanowicz, M. Marzec, J. Niziol, E. Hebda and J. Pielichowski, *Acta Physica Polonica A*, 2012, **121** (2), 485-490.

34 H. Haranczyk, J. Kobierski, J. Niziol, E. Hebda, J. Pielichowski, D. Zalitacz, M. Marzec and A. El-Ghayoury, *J. Appl. Phys.*, 2013, **113** (4), 044702.

35 J. Nizioł, H. Harańczyk, J. Kobierski, E. Hebda, J. Pielichowski and B. Ostachowicz, *J. Appl. Phys.*, 2013b, **114** (14), 144701.

36 J. Nizioł, P. Nowak, J. Kobierski and H. Harańczyk, *European Polymer Journal*, 2015, **66**, 301-306.

37 I. Rau, O. Krupka, J. G. Grote, F. Kajzar and B. Sahraoui, *J. Comput. Met. Sci. Eng.*, 2010, **10**, 531–543.

38 F. M. Zehentbauer, C. Moretto, R. Stephen, T. Thevar, J. R. Gilchrist, D. Pokrajac, K. L. Richard and J. Kiefer, *Spectrochimica Acta Part A: Molecular and Biomolecular Spectroscopy*, 2014, **121**, 147–151.

39 G. K. Ackermann, *Holography: A Practical Approach*, Wiley-VCH, 2007, ISBN 3-527-40663-8.

40 S. C. Gupta, *Textbook on Optical Fiber Communication and its Applications* - Second Edition, PHI Learning Private Limited, New Delhi, April 2012, ISBN-978-81-203-4580-5.